Friction Measurements of Model Saliva-Wine Solutions between Polydimethylsiloxane Surfaces

By

Ryan Edmonds

Thesis

Submitted in partial satisfaction of the requirements for the degree of

Master of Science

in

Chemical Engineering

in the

OFFICE OF GRADUATE STUDIES

of the

UNIVERSITY OF CALIFORNIA

DAVIS

Approved:

Tonya Kuhl, Chair

William Ristenpart

Andrew Waterhouse

Committee in Charge

2020

Contents

Abstract

Evaluation of wine astringency has typically been done by trained sensory panels. In this work, rather than tribometry measurements, the friction of model saliva and model wine mixtures was directly measured using the surface force apparatus (SFA). To mimic the tongue/palate thin films of roughened polydimethylsiloxane (PDMS) were the sliding surfaces. Higher friction forces were observed when sliding in saliva-wine mixtures with higher tannin concentrations. Specifically, friction only increased when saliva-wine complexes were trapped in the contact between the sliding surfaces. These measurements demonstrate that tannin/proline-rich-protein complexes in saliva-wine mixtures reduce lubricity, increase friction, and should correlate with astringency perception.

Acknowledgements

First, I would like to thank my major professor and committee chair, Prof. Tonya Kuhl for her unending support in my research project. Without her contagious enthusiasm, motivation and experience I would not have been able to produce the research presented here. Prof. Kuhl helped me every step of the way from day one and I owe the experience I have gained as a graduate student and researcher to her.

I would also like to thank my committee members: Prof. William Ristenpart and Prof. Andrew Waterhouse for their support of my work and their valuable feedback.

I would like to thank the members of my research group: Tanner Finney for working with me on developing my experimentation and coding skills as well as developing the code used for my data analysis. Michael Bull and Deepshika Gilbile for unending support and for teaching me various important lab and research skills, and for assisting by completing profilometry and AFM measurements.

I would also like to thank Aude Watrelot for her support and guidance throughout my research from start to finish.

I would like to thank Andrew Waterhouse and Patricia Howe in the UC Davis Department of Viticulture and Enology for their contributions of materials for preparing model wine and model saliva solutions.

Last, I would like to thank my parents and sister. There was no end to the support my family provided throughout my studies as not only a graduate student but through all of my studies and I would not be here without them.

1 Introduction

1.1 Quantifying Wine Astringency

Mouth feel and sensory perception of food and beverages has been an area of interest for some time. Research has previously focused on the chemistry and rheology of materials being consumed. Recently, the focus has shifted to the role of surface properties and tribology - the study of friction, wear, and lubrication during oral processing [1, 2, 3]. In particular, food and beverage industries have an interest in mouth tribology and its relation to oral processing as a means to drive product development towards consumer preferences [4]. For example it is common to use sensory panels to evaluate wines when making production decisions. Wine can have a complex sensory profile and one important characteristic of the mouthfeel profile in red wines is astringency, or a drying sensation felt when drinking [3, 5, 6]. While wine characteristics such as pH [7, 8] and ethanol content [9, 10] appear to alter the intensity of astringency, the source of it is related to a group of polyphenols, or condensed tannins also known as polymers of flavanol [6]. Wine tannins play a couple of different roles in generating astringency sensation. First, wine tannins can interact with and bind to proteins in saliva and form complexes, resulting in a decrease in viscosity and in-mouth lubricity [11, 12]. Over time these complexes can cause depletion of the salivary film that is present on mouth surfaces [12, 2]. The result of these interactions is believed to be an increase in friction between the tongue and palate, which is detected by mechanoreceptors in the mouth and not necessarily taste receptors [13]. These findings have sparked interest to quantify wine astringency, especially because high wine grade is positively correlated to tannin and phenolic compounds content [14]. Quantitative studies in the wine industry have shown that the precipitation of these complexes coincides with a loss of lubrication and increase in friction [3]. However, obtaining quantitative measurement of astringency remains challenging. First, appropriate surfaces to mimic the tongue and palate surface must be synthesized. Polydimethylsiloxane (PDMS), a silicon elastomer with well defined properties and

a relatively low Young's Modulus [15] has become widely used for this purpose [3, 16, 13, 2]. PDMS can be spun coated and manipulated in various ways to mimic the roughness of the tongue surface [12]. Due to the complexity of wine and the influence of several chemical parameters on the astringency mouthfeel, [16] model wines are preferred to explore the role of individual wine compounds such as tartaric acid, ethanol, pH and condensed tannins. Artificial saliva can also be synthesized which has been shown to behave similarly to human saliva [12]. These model systems can be used to quantify "mouth feel".

First, appropriate surfaces to mimic the tongue surface must be synthesized. There are numerous pairs of surfaces interacting during oral processing although possibly the most important are tongue-palate and tongue-food interactions [1]. The tongue is a very important muscular organ and has interesting surface characteristics. A human tongue can move at estimated speeds up to 200 mm/s and apply loads between 0.01-90N [17]. It also has a young's modulus on the order of 1kPa, which is quite low [18]. The tongue is covered in papillae that are on the order of 100μm in height. There are two types of tongue papillae: filiform and fungiform. Filiform papillae are the cone shaped structures on the tongue covered with hairs that serve the purpose of "facilitating movement between the tongue and food" [19], while fungiform papillae are between the filiform structures and show the taste buds [19]. It is important to mimic the young's modulus and surface asperities of the tongue, as even its deformation during oral processing may contribute to mouthfeel. Polydimethylsiloxane (PDMS), a silicon elastomer with well defined properties and a relatively low Young's Modulus [15] has become widely used for this purpose [3, 16, 13]. PDMS can be spun coated and manipulated in various ways to mimic the tongue surface [12]. Wine composition is well understood and model wines can be prepared and tailored to explore the attributes of different compositions [16]. Artificial saliva can also be synthesized which has been shown to behave similarly to human saliva [12]. These model systems can be used to quantify "mouth feel".

1.2 Previous Work

Previous studies have confirmed the relationship between wine astringency and the formation of complexes [11, 20]. One study correlated turbidity measurements and haze formation with a mixture of saliva and tannic acid to astringency perception through sensory panels [20]. In a recent study Watrelot et al. completed detailed chemical analysis of wines and their tannins. This explicitly demonstrated that increased tannin size and turbidity of wines mixed with different proteins as well as human saliva increased the sensory perception of dryness of model and commercial wines [5]. Zanchi et al. completed an extensive study of the mechanism and structure of protein-tannin complex formation [11]. These studies support the idea that the formation and precipitation of complexes results in a decrease in lubricity and increased friction, but there are few studies which endeavor to quantify astringency in the context of friction. The most comprehensive work was done by Brossard et al. which measured the friction coefficient of different red wine-saliva mixtures at various normal loads and velocities by sliding steel balls across PDMS substrates using a modified ball on disc tribometer [3]. They demonstrated an increase in friction coefficient for saliva-wine mixtures when compared to saliva alone. A recently published study by Wang et al. compared various tribological measurements of high tannin model wines and human saliva to sensory results [2]. They described astringency with the categories of rough, pucker and dry. Pucker and drying were related to the acidity and tannin content, respectively. The work showed that rough appeared to be dependent on the perception of dry and pucker. Finally, Watrelot et al. conducted a surface force apparatus (SFA) study comparing friction forces of saliva, low tannin wines, and high tannin wines between ultra-smooth hydrophilic mica and hydrophobic PDMS surfaces [16]. This study surprisingly found lower friction with high tannin wines. It was hypothesized that the low friction was due to the exclusion of saliva-wine complexes from between the smooth sliding surfaces [16]. This study continues the work of Watrelot et

al. with rougher PDMS surfaces and friction measurements in the presence of model saliva and model wine solutions with low and high grape tannin concentrations corresponding to commercial wines.

1.3 Surface Force Apparatus

The Surface Force Apparatus (SFA) has a normal and lateral distance sensitivity of 0.1nm and 1μm. The SFA is also capable of a high force sensitivity of $10^{-8}N$ by implementing various springs with known spring constants and easily measurable displacements [21]. In order to have smooth surfaces and generate fringes of equal chromatic order (FECO) a freshly cleaved layer of mica is silvered and then glued mica side up to a disk with a cylindrical geometry. The SFA utilizes a cross cylinder geometry for it's surfaces because local contacts are identical to a sphere on flat geometry while allowing maximization of potential contact points for measurements. At this point, a film may be deposited on top of the mica using a variety of techniques. This research focuses on spin coating PDMS films onto the surfaces, and the detailed procedure will be described later. In the SFA, white light is directed up through the surfaces, and due to the silver layers only specific wavelengths constructively interfere and emerge.

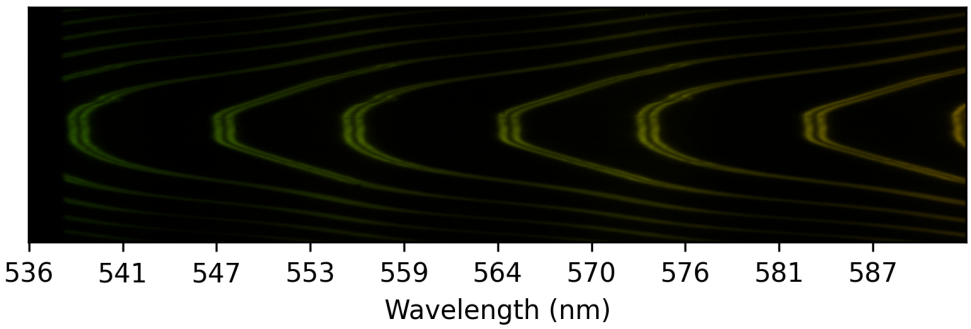

Figure 1: Fringes of Equal Chromatic Order observed for a contact between two PDMS surfaces.

The constructive interference can be visualized and measured as fringes of equal chromatic

order (FECO) by focusing the light out of the surfaces onto the slit of a grating spectrometer [21] (Figure 1). The shape of the fringes gives qualitative information about the contact and can also be used to determine area of contact and the separation distant between the surfaces. There are additional attachments for the SFA that allow for the lateral sliding of the bottom surface. The bimorph slider (Figure 4) is attached to the bottom surface assembly and is constructed of a piezoelectric material. When a voltage is applied to the bimorph, it undergoes displacement and moves the bottom surface laterally. Applying specified voltage waveforms enables the surface to slide at desired velocities [22]. Springs with a strain gauge connected to the top surface can then be used to measure the friction force between the surfaces.

1.4 Surface Force Apparatus Optic Theory

Quantitative measurements of the wavelengths of the FECO fringes combined with optic theory of fringes [23] enables determination of film thickness. The first step in this process is to prepare surfaces for SFA with only silvered mica and no deposited PDMS film. These surfaces are then mounted inside the SFA to determine mica thickness and contact. These FECO fringes can be imaged (figure 2a) for analysis. After this the same experiment is completed with PDMS films spun coated onto the same mica surfaces and the fringe position in contact can be imaged again (figure 2b). The fringes shift to higher wavelengths due to the deposited polymer film. Figure 2 illustrates this change in fringe wavelength.

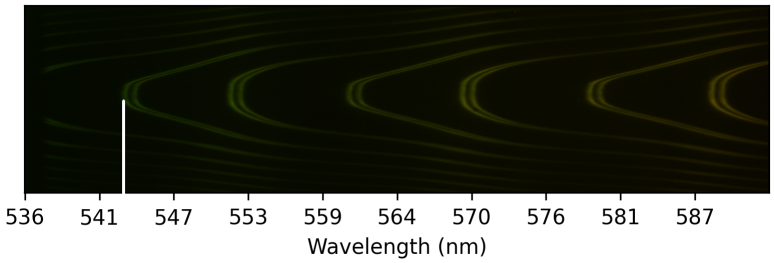

(a) Contact FECO fringes for a Mica.

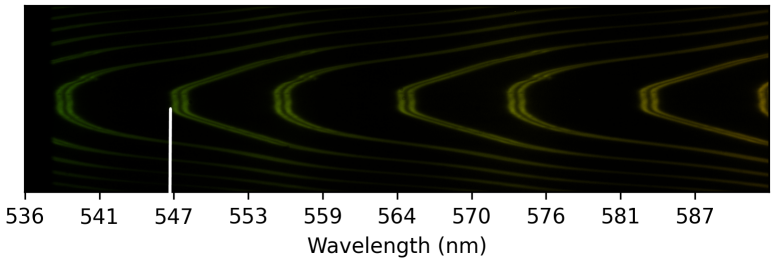

(b) Contact FECO fringes for PDMS spin coated onto Mica.

Figure 2: FECO Fringes for surfaces before and after spin coating PDMS. Vertical white line represents a specific fringe being tracked.

Multiple beam interferometry and optical analysis can be used to determine absolute properties of the various layer's thickness and refractive index. However, previous work [23] has derived the appropriate equations to determine the thickness of the film within ≤ 1 % based on the shift in wavelength as illustrated in Figure 2. For example, the contact of FECO wavelength in the absence of a film of a single fringe is λ, and the change in wavelength from the contact with polymer is $\Delta\lambda_n$. Using the fringe position, refractive index of the layers (μ_1 is the refractive index of mica and μ_2 is the refractive index of PDMS), equation (1) enables the total film thickness, D, to be determined.

$$tan\left(k\mu_2 2D\right) = \frac{2\bar{\mu} sin\left(n\pi\Delta\lambda_n/\lambda\right)}{\left(1+\bar{\mu}^2\right) cos\left(n\pi\Delta\lambda_n/\lambda\right) + \left(\bar{\mu}^2 - 1\right)} \tag{1}$$

Where

$$k = \frac{2\pi}{\lambda} \tag{2}$$

and

$$\bar{\mu} = \frac{\mu_1}{\mu_2} \tag{3}$$

This equation can be solved for D:

$$D = \left(\frac{\lambda}{4\pi\mu_2}\right) atan\left(\frac{2\bar{\mu} sin\left(n\pi\Delta\lambda_n/\lambda\right)}{\left(1+\bar{\mu}^2\right) cos\left(n\pi\Delta\lambda_n/\lambda\right) + \left(\bar{\mu}^2 - 1\right)}\right) \tag{4}$$

2 Materials and Methods

2.1 Surface Preparation

PDMS (Sylgard 184 Silicon Elastomer Kit, Dow Corning) was deposited in a volume of 0.25 mL in hexanes (Fisher Chemical, ACS, 98.5%+, mixed isomers) and spun coated onto silicon wafer pieces at 6000 rpm for 150 seconds to determine the thickness vs. concentration for Sylgard 184 with 10:1 base to curing agent ratio (Figure 3. Several films were prepared each with a different PDMS concentration and the film thickness was measured using a Dektak 150 Surface Profiler. A PDMS concentration of 20 g/L was selected to yield 40 nm films. To make the SFA substrates back silvered (55 nm) sheets of equal thickness mica (2-3 μm) were glued onto cylindrically curved silica disks (R=1.5 cm) using an ultraviolet light curing glue (Norland Optical Adhesive 61). The glue was cured in a UV-Ozone device (UVO Cleaner Model 342) with three 5 minute curing cycles, with 5 minute breaks in-between. Thin films of PDMS were then deposited on the mica by spin coating with 20 g/L PDMS in toluene (Fisher Chemical, Certified ACS) at 6000 rpm for 150 seconds. The samples were then cured for a minimum of 48 hours under vacuum at 70°C.

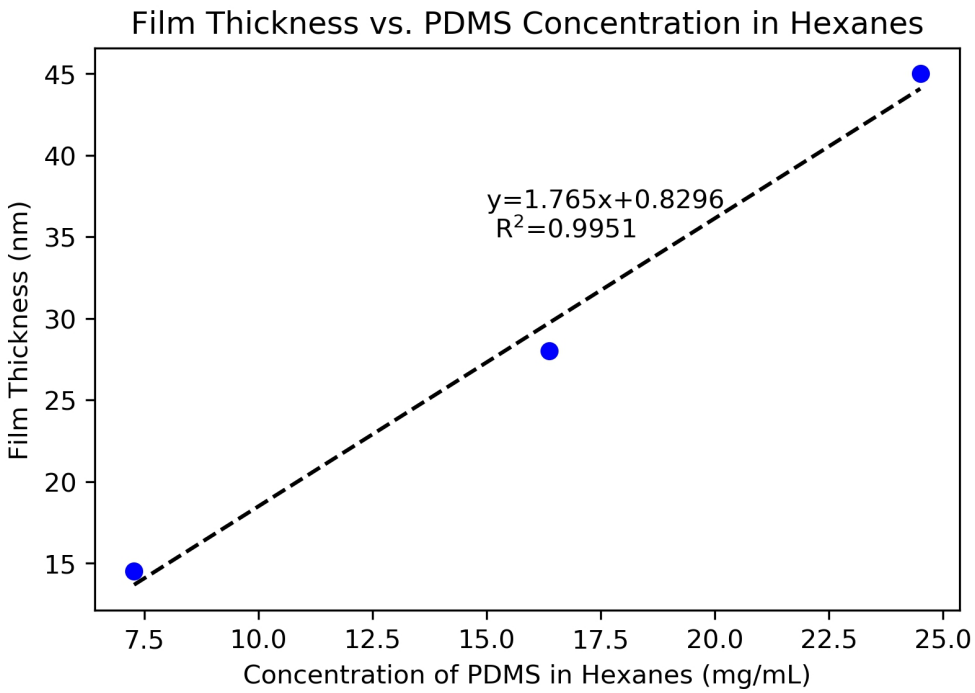

Figure 3: Spin curve for PDMS thin films spun at 6000 RPM for 150 seconds on silicon substrates.

To mimic the tongue/palate, the thin films of PDMS were roughened following a procedure previously published by Choi et al. [24]. After curing, the surfaces were placed in a toluene bath for 24 hours. The surfaces were then returned to the oven at 70 °C under vacuum for a minimum of 48 hours to drive off residual solvent. Surface topography was measured by Michael Bull, a member of the Kuhl Research Group, using an atomic force microscope (Veeco Multimode Nanoscope III, Olympus AC240 tip, tapping mode). The roughened PDMS surfaces exhibited a root mean square roughness of 3.44 nm. The water contact angle on roughened PDMS had an advancing angle of θ_{adv}=111±4° and a receding angle of θ_{rec}=70±3°.

Component	Concentration(g/L)
KH_2PO_4 (Fisher Scientific, Certified ACS)	0.626
NaCl (Fisher Scientific, Certified ACS)	1.594
KCl (Fisher Scientific, Certified ACS)	0.202
Uric Acid (Millipore Sigma, HPLC)	0.021
Urea (Fisher Scientific, Certified ACS)	0.198

Table 1: Composition of model saliva solution excluding protein [25]

2.2 Model Solution Preparation

Model wines with low and high tannin concentrations corresponding to commercially produced wines were prepared. First, solutions of 12% ethanol (Koptec 200 proof pure ethanol, anhydrous) in ultra purified water ($\geq$18MΩ) were prepared. Tartaric acid (Sigma Aldrich, ACS Grade) was added to the solutions to a concentration of 5g/L. Commercial grape tannin (Tannin VR Grape, Biotan, Laffort) was added to the solutions to a concentration of 0.2g/L and 1g/L for low (LT) and high (HT) tannin wines, respectively. The pH of these solutions was then adjusted to 3.5 (Fisher Scientific Accumet Basic Ab15 Plus pH meter) using sodium hydroxide (Fisher Scientific, Certified ACS) solution in water. Model wine solutions were stored under refrigeration and used within one week.

The model saliva (MS) solution was prepared according to the procedure previously published by Sarkar et al. [25]. Briefly, a solution of ultra purified water containing potassium dihydrogen phosphate, sodium chloride, potassium chloride, uric acid and urea was prepared as described in Table 1. Protein (Poly-l-proline, Millipore Sigma, MW 1,000-10,000) was added at a concentration of 0.5g/L. Model saliva solutions were stored at -20°C until use.

2.3 Surface Force Apparatus

The SFA technique has been used extensively to measure interaction forces and friction/lubrication properties of thin-film samples between surfaces [26, 27, 22, 28]. The PDMS coated surfaces

were mounted in a crossed-cylinder configuration (Figure 4). This configuration is locally equivalent to a sphere on a flat geometry as the surface separation D was far smaller than the surface curvature. The absolute separation distance (D) between the two mica surfaces was directly determined by multiple beam interferometry (MBI) based on interference fringes of equal chromatic order (FECO) [23]. FECO were produced by passing white light through the opposing surfaces, and imaged in a 3/4 meter grating spectrometer (Acton, Teledyne Princeton Instruments, New Jersey, USA). A custom automated SFA Mark-II was used for data collection with a bimorph slider and friction device (SurForce, Santa Barbara, CA). A sensitive CCD camera (Princeton SPEC-10:2K Roper Scientific, Trenton, NJ) was interfaced with the spectrometer and computer acquisition system to allow automated FECO wavelength determination [29, 23].

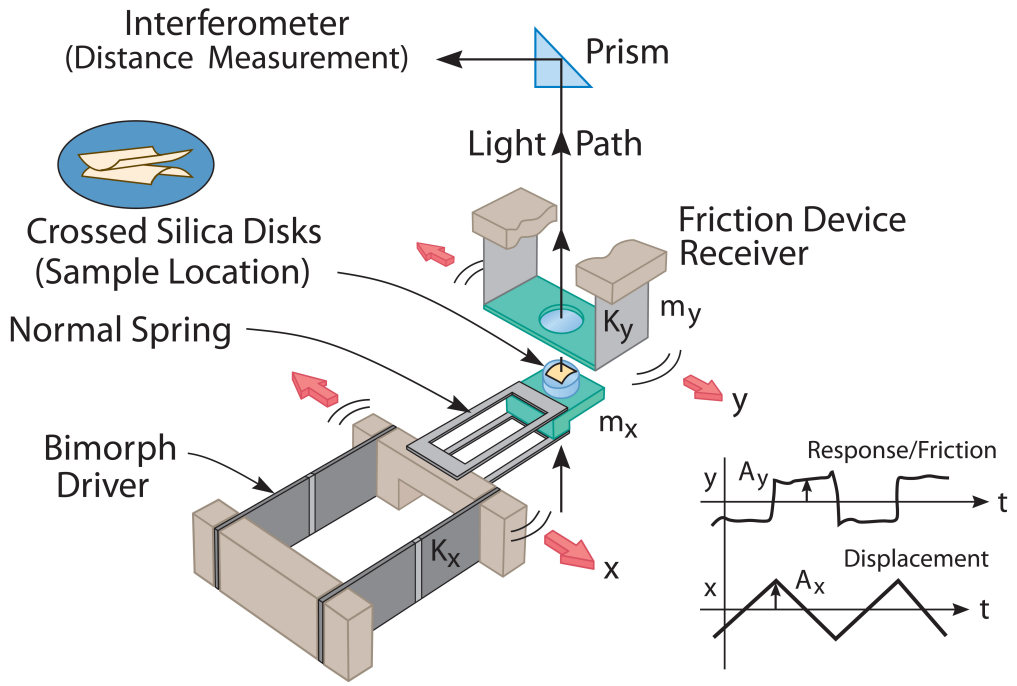

Figure 4: Surface forces apparatus friction experimental setup. The SFA allows the shearing of two surfaces in contact and can measure the friction force at varying sliding velocities and normal loads. The bimorph driver receives a saw-tooth voltage (graph) to translate/displace the lower surface back and forth at a specified velocity. The friction device receiver is a vertical spring system with semi-conductor strain gauges to measure the frictional response. Adapted from [22]

Measurements were conducted in a temperature controlled room at 30°C to match mouth temperature when drinking [30]. A petri dish with water was placed in the SFA box with the samples to help limit evaporation of model solutions. PDMS thickness measurements were determined by bringing the surfaces into contact in air before injecting solutions. The thickness of the PDMS films after roughening ranged from 15-30 nm.

In all experiments the friction of model saliva (MS) solution was measured first. Approximately 15μL of solution was injected between the surfaces and left for at least 45 minutes prior to commencing measurements. The incubation with MS allowed a protein adsorption layer to form so that MS ultimately wetted the substrates to mimic the oral surface. Sliding velocities were 0.50, 2.5, 5.0, 25, and 50 μm/s. Normal loads were applied across a range of 0 to 1.1 mN. In most experiments the same contact position was used with MS, then the 50:50 mixture of MS and low tannin wine (LT), and finally a 50:50 mixture of MS and high tannin wine (HT). When changing to a new solution, the surfaces were rinsed with fresh model saliva. After injection of each mixture, the surfaces were placed in soft contact and imaged from above (Edmund Optics EO-5012C 1/2" CMOS Color USB Camera). Friction was measured through recording the deflection of the vertical spring system holding the top surface using an integrated strain gauge.

2.4 Data Analysis

For each normal force, 6-20 lateral slides were completed at each sliding velocity. Friction measurements were conducted for the same contact position in each lubricant. These measurements were completed in triplicate with new surfaces for each experiment. Friction data was calculated using ImageJ as well as custom written Python code. Average friction forces reported were calculated using inverse variance weighting. Friction data was calculated using ImageJ as well as custom written Python code. The error reported for slopes of friction force vs. normal load plots is standard error from weighted linear regression.

3 Results and Discussion

Initial measurements in each experiment were done with model saliva (MS). Afterwards, the friction forces of the mixture of MS and model wines with low (LT) and then high (HT) concentrations of grape tannins were carried out. As shown in Figure 5, the friction force vs. load (normal force) was always lowest in MS and showed a linear trend. In all cases, only a modest increase in friction force was observed upon increasing the velocity from 5 to 50 μm/s (Figure 5a and Figure 5b). The friction coefficient (in MS μ=0.13±0.05 and 0.21±0.03 respectively) was obtained from the slope, $\mu=\frac{dF}{dL}$. After MS measurements, LT was added to the system. For both sliding velocities (Figure 5), LT exhibited a higher fiction coefficient(μ=0.48±0.08 and 0.51±0.16) than MS. After a rinsing the surfaces with fresh MS, HT was injected. Measurements showed the highest friction coefficient with HT (μ=0.71±0.17 and 0.88±0.15).

(a)

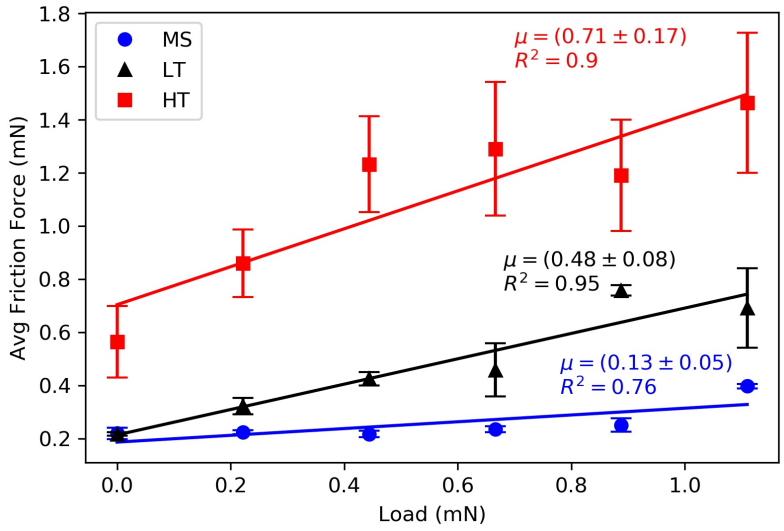

(b)

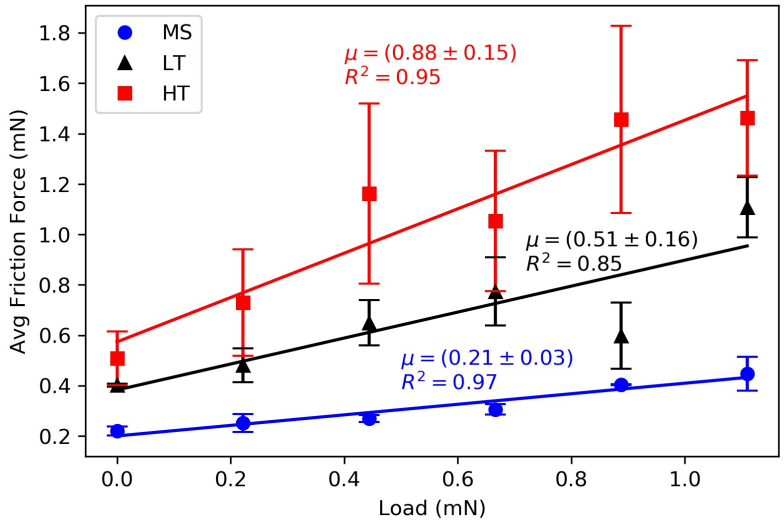

Figure 5: Friction force vs. normal load at sliding velocities of (a) 5 μm/s and (b) 50μm/s. MS is model saliva; LT is low tannin model wine; and HT is high tannin model wine. Lines are linear fits to the data to determine the friction coefficient $\frac{dF}{dN} = \mu$.

When considering tannin concentration, HT exhibited the highest friction at all sliding velocities, followed by LT. Both saliva-wine mixtures had higher friction than MS alone. As seen in Figure 6a, the friction force increased with sliding velocity up to approximately 5μm/s. Above this velocity there is little dependence of friction force on sliding velocity, even at different normal loads. When sliding under a higher normal load (figure 6b), the friction

force increased for both LT and HT, compared to only MS. The increasing trends of friction force with tannin concentration are consistent with previous findings with a ball on disc tribometer [3, 31, 32].

In contrast to these findings, previous SFA studies by Watrelot et al. did not observe increasing friction with increasing tannin concentration using human saliva, model, and commercial wines [16]. The authors' hypothesized that the lower friction in high tannin wine was due to the exclusion of grape tannin/proline-rich-protein complexes from between the smooth sliding surfaces. In the work here with rough PDMS surfaces, complexes formed were visible when viewing the sliding contact region from above with a microscope. These complexes closely align with the representations provided by Brossard et al. [3].

When observing the contact with LT mixture present as the lubricant, there were obvious complexes in solution, though only a slight increase in surface deposited material was observed. The HT mixture resulted in a larger area with a multitude of deposited material from solution. The saliva-wine mixtures also exhibited visual cloudiness. Figure 7 displays images taken of sliding contacts in MS, LT, and HT. The contact in MS shows minimal material adsorbed to the surface. The contact in LT shows some increase in surface material, but still appears generally smooth. Finally, HT shows further change, including a ripple-like texture throughout the area as well as a general increase in material and non-uniformity. In saliva, many proteins other than poly-L-proline exist as well as other compounds that can lead to different reactivity with wine components [20]. Clearly, the roughened PDMS surfaces were able to trap/adsorb the complexes resulting in higher friction compared to previous work by Watrelot et al. [16]. There are other factors as well that potentially contributed to differing results from the previous study. First, this study utilized a different ratio of MS to model wine in friction experiments. Second, Watrelot et al. also investigated human saliva and commercial wines.

(a)

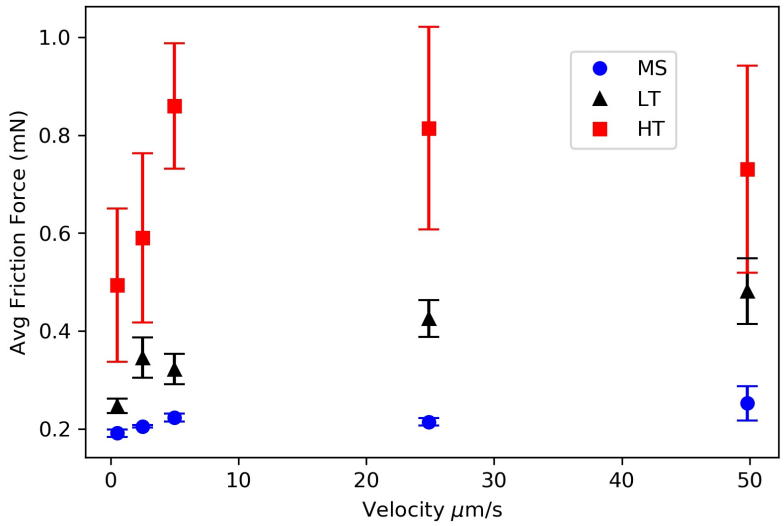

(b)

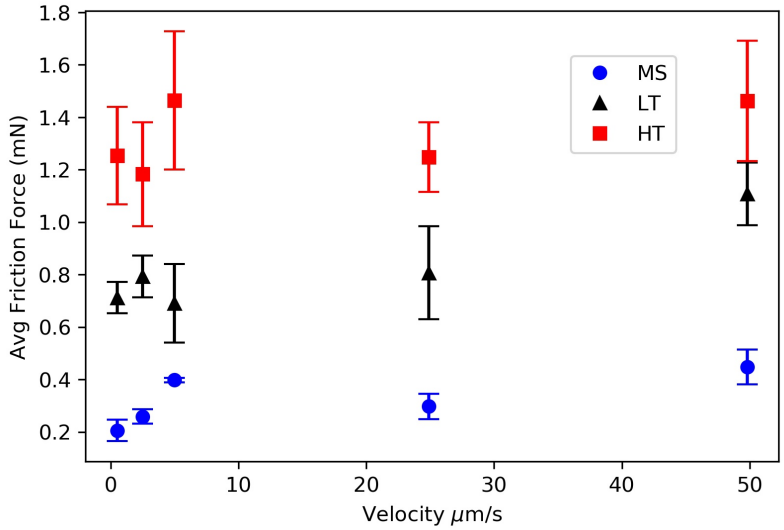

Figure 6: Friction force vs. sliding velocity at normal loads of (a) 0.22 mN and (b) 1.11 mN with model saliva (MS) and model wine mixtures (LT, HT)

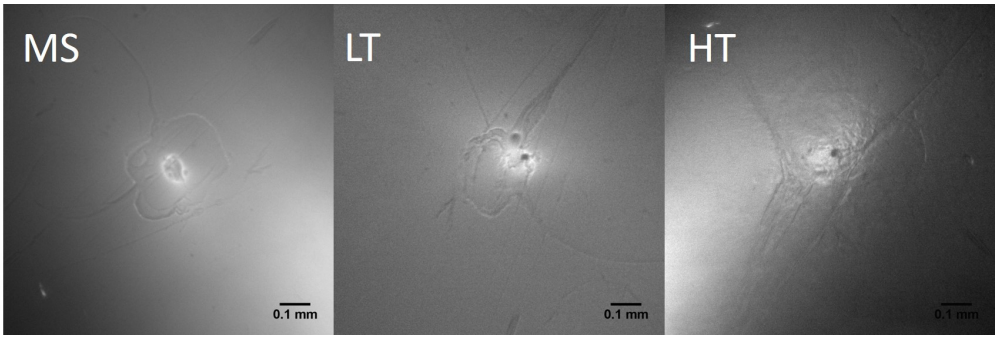

Figure 7: Images of contacts during SFA experiments in different model saliva (MS) and models wine mixtures (LT, HT).

The adsorption/trapping of model saliva-wine complexes between the sliding surfaces were further quantified by thickness measurements in the SFA which showed an increase after injection of each solution between the surfaces (Table 2). All thickness changes reported are in reference to dry PDMS contact in air. After adding MS, the thickness increased by 15-120 nm under a low load, and 1-70 nm in hard flattened contact. After adding LT between the surfaces the thickness increased by 55-190 nm at low load and 18-70 nm in hard flattened contact. Injecting HT between the surfaces with MS showed the largest increase at low load on the order of 500nm. At hard contact, HT also showed the largest increase: 34-105 nm. These changes in thickness further confirm the presence of saliva-wine complexes trapped in the contact which are believed to be the cause of increased friction [16].

Solution	Contact Type	Increased Thickness (nm)
MS	Low load	15-120 nm
MS	Hard Flattened Contact	1-70
LT	Low Load	55-190
LT	Hard Flattened Contact	18-70
HT	Low Load	500
HT	Hard Flattened Contact	34-105

Table 2: Change in thickness corresponding to solutions injected between PDMS surfaces. MS is model saliva; LT is low tannin model wine; HT is high tannin model wine.

The role of adsorbed complexes was further confirmed in a separate experiment by taking measurements where HT was measured before switching to LT. Even with rinsing with MS,

adsorbed saliva-wine complexes remained and the measured friction force of the subsequent LT was very similar to HT. Measurements were also taken in which contacts with fewer adsorbed complexes were chosen, and results were similar to that of Watrelot et al. where low tannin wine exhibited higher friction than high tannin wine [16]. This further confirms that the saliva-wine complexes adsorbed or trapped on the surface at the sliding contact have a strong influence on the friction observed. Finally, the data for LT and HT were compared by normalizing the friction force to that of MS at the same experimental conditions. This ratio allows for a comparison to baseline lubrication with only MS between the surfaces. Normalized friction force increased with increased tannin concentration, supporting the claim of a loss of lubrication [3, 33]. With the exception of the sliding velocity of 50μm/s, the high tannin mixture had higher normalized friction than the low tannin mixture (figure 8). A likely cause for this lower normalized friction in HT at the highest sliding velocities was again visible squeeze out of complexes from the contact.

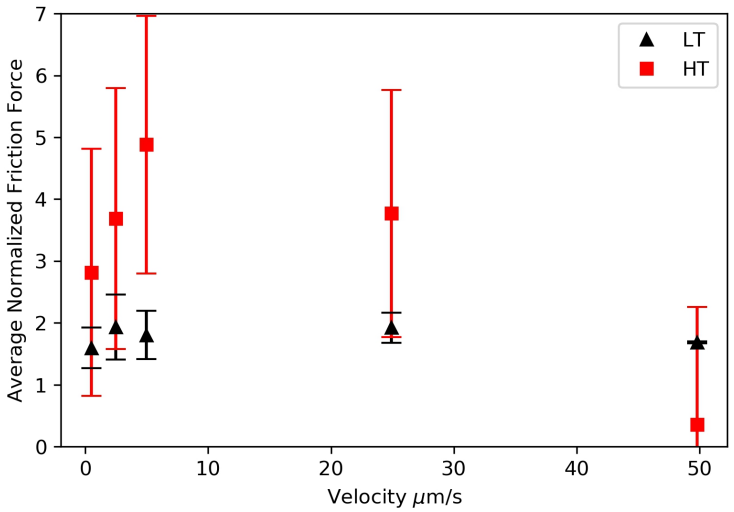

Figure 8: Normalized friction force vs. sliding velocity at a normal load of 1.11mN

In wine, tannins interact with proteins and are mainly responsible for the astringency perception, but there are also several other species present in wine that can modify the final astringency perception [9]. These factors can explain the differences in friction results as

well as complexes formed during experiments between this and the previous study. Future work will investigate human saliva and commercial wines.

In conclusion, this study demonstrates a method towards a robust, quantitative measure of wine friction that could be used as a measure of astringency [3, 16, 32, 31]. Surfaces were coated with PDMS and roughened by solvent exposure to mimic the tongue/palate surface for SFA friction experiments. The measurements showed that friction force increased with tannin concentration in model wine-saliva mixtures. The tannins in wine interacted with proteins in saliva to form complexes that aggregated out of solution and decreased lubrication [33, 3]. Importantly, the friction force increased with tannin concentration only when complexes were trapped in the contact. When the complexes were excluded, lubrication improved and friction forces decreased.

References

[1] Jianshe Chen and Jason R. Stokes. Rheology and tribology: Two distinctive regimes of food texture sensation. *Trends in Food Science and Technology*, 25(1):4–12, 2012.

[2] Shaoyang Wang, Sandra M. Olarte Mantilla, Paul A. Smith, Jason R. Stokes, and Heather E. Smyth. Astringency sub-qualities drying and pucker are driven by tannin and pH – Insights from sensory and tribology of a model wine system. *Food Hydrocolloids*, 109(June), 2020.

[3] Natalia Brossard, Huifang Cai, Fernando Osorio, Edmundo Bordeu, and Jianshe Chen. "Oral" Tribological Study on the Astringency Sensation of Red Wines. *Journal of Texture Studies*, 47(5):392–402, 2016.

[4] Jason R. Stokes, Michael W. Boehm, and Stefan K. Baier. Oral processing, texture and mouthfeel: From rheology to tribology and beyond. *Current Opinion in Colloid and Interface Science*, 18(4):349–359, 2013.

[5] Aude A. Watrelot, Hildegarde Heymann, and Andrew L. Waterhouse. Red Wine Dryness Perception Related to Physicochemistry. *Journal of Agricultural and Food Chemistry*, 68(10):2964–2972, 2020.

[6] M. Medel-Marabolí, J.L. Romero, E. Obreque-Slier, A. Contreras, and A. Peña-Neira. Effect of a commercial tannin on the sensorial temporality of astringency. *Food Research International*, 102:341 – 347, 2017.

[7] S. Kallithraka, J. Bakker, and M. N. Clifford. Effect of pH on Astringency in Model Solutions and Wines. *Journal of Agricultural and Food Chemistry*, 45(6):2211–2216, 1997.

[8] Martino Forino, Luigi Picariello, Alessandra Rinaldi, Luigi Moio, and Angelita Gambuti. How must ph affects the level of red wine phenols. *Lebensmittel-Wissenschaft + [i.e. und]*

Technologie. Food science + technology. Science + technologie alimentaire, 129:109546, 2020.

[9] Stéphane Vidal, Philippe Courcoux, Leigh Francis, Mariola Kwiatkowski, Richard Gawel, Pascale Williams, Elizabeth Waters, and Véronique Cheynier. Use of an experimental design approach for evaluation of key wine components on mouth-feel perception. *Food Quality and Preference*, 15(3):209–217, 2004.

[10] Lukas Danner, Jun Niimi, Yuxing Wang, Marcell Kustos, Richard A. Muhlack, and Susan E. P. Bastian. Dynamic viscosity levels of dry red and white wines and determination of perceived viscosity difference thresholds. *American Journal of Enology and Viticulture*, 70(2):205–211, 2019.

[11] D. Zanchi, C. Poulain, P. Konarev, C. Tribet, and D. I. Svergun. Colloidal stability of tannins: Astringency, wine tasting and beyond. *Journal of Physics Condensed Matter*, 20(49), 2008.

[12] Laura Laguna and Anwesha Sarkar. Oral tribology: update on the relevance to study astringency in wines. *Tribology - Materials, Surfaces and Interfaces*, 11(2):116–123, 2017.

[13] Rutuja Upadhyay, Natalia Brossard, and Jianshe Chen. Mechanisms underlying astringency: Introduction to an oral tribology approach. *Journal of Physics D: Applied Physics*, 49(10), 2016.

[14] Meagan D. Mercurio, Robert G. Dambergs, Daniel Cozzolino, Markus J. Herderich, and Paul A. Smith. Relationship between red wine grades and phenolics. 1. Tannin and total phenolics concentrations. *Journal of Agricultural and Food Chemistry*, 58(23):12313–12319, 2010.

[15] Abel L Thangawng, Rodney S Ruoff, Melody A Swartz, and Matthew R Glucksberg. An ultra-thin PDMS membrane as a bio / micro – nano interface : fabrication and characterization. *Biomed Microdevices*, pages 587–595, 2007.

[16] Aude A. Watrelot, Tonya L. Kuhl, and Andrew L. Waterhouse. Friction forces of saliva and red wine on hydrophobic and hydrophilic surfaces. *Food Research International*, 116(February):1041–1046, 2019.

[17] Clementine Pradal and Jason R. Stokes. Oral tribology: Bridging the gap between physical measurements and sensory experience. *Current Opinion in Food Science*, 9:34–41, 2016.

[18] D. M. Dresselhuis, E. H.A. de Hoog, M. A. Cohen Stuart, and G. A. van Aken. Application of oral tissue in tribological measurements in an emulsion perception context. *Food Hydrocolloids*, 22(2):323–335, 2008.

[19] H. Ranc, A. Elkhyat, C. Servais, S. Mac-Mary, B. Launay, and Ph Humbert. Friction coefficient and wettability of oral mucosal tissue: Changes induced by a salivary layer. *Colloids and Surfaces A: Physicochemical and Engineering Aspects*, 276(1-3):155–161, 2006.

[20] Caterina Dinnella, Annamaria Recchia, Giovanna Fia, Mario Bertuccioli, and Erminio Monteleone. Saliva characteristics and individual sensitivity to phenolic astringent stimuli. *Chemical Senses*, 34(4):295–304, 2009.

[21] Jacob N. Israelachvili. Chapter 12 - force-measuring techniques. In Jacob N. Israelachvili, editor, *Intermolecular and Surface Forces (Third Edition)*, pages 223 – 252. Academic Press, San Diego, third edition edition, 2011.

[22] J. Israelachvili, Y. Min, M. Akbulut, A. Alig, G. Carver, W. Greene, K. Kristiansen, E. Meyer, N. Pesika, K. Rosenberg, and H. Zeng. Recent advances in the surface forces apparatus (SFA) technique. *Reports on Progress in Physics*, 73(3), 2010.

[23] J. N. Israelachvili. Thin film studies using multiple-beam interferometry. *Journal of Colloid And Interface Science*, 44(2):259–272, 1973.

[24] Gun Young Choi, Soojin Kim, and Abraham Ulman. Adhesion Hysteresis Studies of Extracted Poly(dimethylsiloxane) Using Contact Mechanics. *Langmuir*, 13(23):6333–6338, 2002.

[25] Anwesha Sarkar, Kelvin K.T. Goh, and Harjinder Singh. Colloidal stability and interactions of milk-protein-stabilized emulsions in an artificial saliva. *Food Hydrocolloids*, 23(5):1270–1278, 2009.

[26] Jimmy Faivre, Buddha Ratna Shrestha, Guojun Xie, Thierry Delair, Laurent David, Krzysztof Matyjaszewski, and Xavier Banquy. Unraveling the Correlations between Conformation, Lubrication, and Chemical Stability of Bottlebrush Polymers at Interfaces. *Biomacromolecules*, 18(12):4002–4010, 2017.

[27] Jacob N. Israelachvili and Gayle E. Adams. Measurement of forces between two mica surfaces in aqueous electrolyte solutions in the range 0-100 nm. *Journal of the Chemical Society, Faraday Transactions 1: Physical Chemistry in Condensed Phases*, 74:975–1001, 1978.

[28] Jacob N. Israelachvili and Patricia M. McGuiggan. Adhesion and short-range forces between surfaces. part i: New apparatus for surface force measurements. *Journal of Materials Research*, 5(10):2223–2231, 1990.

[29] Daniel F. Kienle and Tonya L. Kuhl. Analyzing refractive index profiles of confined fluids by interferometry. *Analytical Chemistry*, 86(23):11860–11867, 2014.

[30] P. M. Michailesco, J. Marciano, A. R. Grieve, and M. J.M. Abadie. An in vivo recording of variations in oral temperature during meals: A pilot study. *The Journal of Prosthetic Dentistry*, 73(2):214–218, 1995.

[31] J. H.H. Bongaerts, D. Rossetti, and J. R. Stokes. The lubricating properties of human whole saliva. *Tribology Letters*, 27(3):277–287, 2007.

[32] J. F. Prinz and P. W. Lucas. Saliva tannin interactions. *Journal of Oral Rehabilitation*, 27(11):991–994, 2008.

[33] Jacqui M Mcrae and James A Kennedy. Wine and Grape Tannin Interactions with Salivary Proteins. *Molecules*, 16:2348–2364, 2011.